10-YEARS OPERATIONAL GOME/ERS-2 TOTAL COLUMN PRODUCTS: THE GDP 4.0 ALGORITHM

Diego Loyola[(1)], Michel Van Roozendael[(2)], Robert Spurr[(3)], Dimitris Balis[(4)], Jean-Christopher Lambert[(2)], Yakov Livschitz[(1)], Pieter Valks[(1)], Thomas Ruppert[(1)], Pepijn Kenter[(5)], Caroline Fayt[(2)], Claus Zehner[(6)], Bernd Aberle[(1)], and Sander Slijkhuis[(1)].

(1) DLR, Oberpfaffenhofen, D-82234 Wessling, Germany
(2) BIRA, Avenue Circulaire 3, 1180 Bruxelles, Belgium
(3) RT Solutions, Inc., 9 Channing Street, Cambridge MA 02138, United States
(4) Aristotle University of Thessaloniki, Box 149, 54124 Thessaloniki, Greece
(5) Science & Technology BV, PO Box 2608, 2600 AP, Delft, The Netherlands
(6) ESA, Via Galileo Galilei CP. 64, 00044 Frascati, Italy

ABSTRACT

GOME has become an important instrument for trace gases trend analysis, with a data record now exceeding ten years duration. The GOME Data Processor (GDP) operational retrieval algorithm has generated total ozone and NO_2 columns, as well as cloud parameters since July 1995. This paper presents the GDP version 4.0 algorithm, a major upgrade to the operational system. The GDP 4.0 retrieval algorithm uses an optimized DOAS (Differential Optical Absorption Spectroscopy) algorithm; least-squares slant column fitting is followed by Air Mass Factor (AMF) conversions to generate vertical columns. GDP 4.0 has improved wavelength calibration and reference spectra, and includes a new molecular Ring correction scheme to deal with the distortion of ozone absorption features due to inelastic Raman scattering effects. The AMFs are calculated on-line using the pseudo-spherical multiple-scattering radiative transfer code LIDORT and adjusted iteratively to reflect the fitted slant column result. GDP 4.0 includes accurate cloud parameter estimation using the cutting-edge cloud correction algorithms OCRA and ROCINN. The geophysical validation demonstrated the long-term stability of the GDP 4.0 total column ozone, reaching an accuracy comparable to that obtainable from ground-based sensors.

1. INTRODUCTION

1.1 GOME Ground Segment

The GOME Data Processor (GDP) project was initiated at DLR in 1992, and comprises the operational off-line and near-real-time ground segment for GOME with modules for data ingestion and archiving, Level 1 and Level 2 product generation, quality assurance, product catalogue and dissemination [1]. The ground segment is completed with the GOME value added products (Level 3 and Level 4). The first versions of the GDP level 0-to-1 and level 1-to-2 systems were ready a few months after the launch of GOME; the complete processing chain including systematic product distribution is running operational since early 1996.

1.2 GDP 0-to-1 System

GOME raw data is converted into calibrated and geolocated radiances using the GDP 0-to-1 processor by the application of a series of calibration algorithms. In-flight observations of dark current, wavelength calibration lamp, LED and Sun measurements are used for signal correction (dark current and pixel-to-pixel gain), spectral and radiometric calibration, polarization correction, geolocation and quality assessment [6]. The current operational version 2.2 of the GDP 0-to-1 processor was released in April 2002. A new GDP 0-to-1 version is currently under preparation, the main algorithm improvements will be related to polarization correction and wavelength estimation. After validation/verification the complete GOME data record will be reprocessed and the products will be distributed on-line via a dedicated FTP server by end of 2006. As discussed in Section 2.4, the long-term monitoring of the GDP computed in-flight calibration parameters as well as on the degradation correction (Fig.1) for the level 1 spectra is especially important.

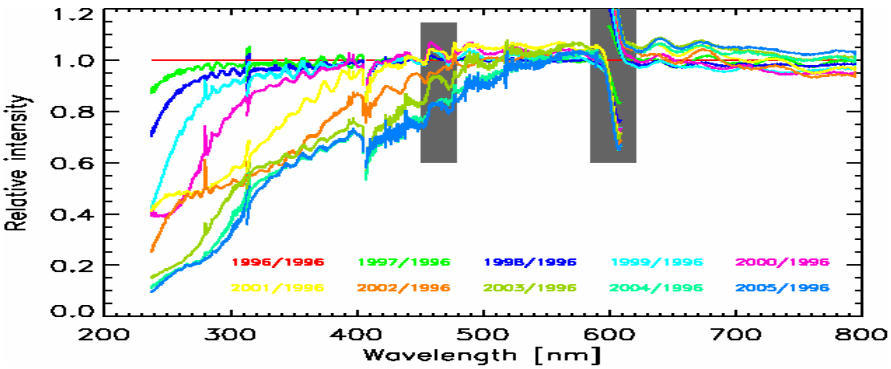

Fig.1. Ratio of the Sun Mean reference spectra measured by GOME showing the instrument degradation.

1.3 GDP 1-to-2 System

The present GDP 1-to-2 version 4.0 has been released in December 2004. The GDP 4.0 algorithm was implemented in the UPAS system at DLR, the new operational environment for GOME and GOME-2. The algorithm is described in detail in Section 2. Independent validation showed that the total ozone accuracy reached by GDP 4.0 is at the *percentage level*, i.e. it is comparable to the accuracy of the ground-based instruments [20].

1.4 GOME Near-Real-Time Service

The need of providing a NRT service was identified at the early days of GOME. The first GOME NRT service was already established in January 1997 with the installation of GDP in the core ERS-2 stations: Kiruna, Gatineau (includes also data from Prince-Albert) and Maspalomas. ESA has extended the number of receiving stations since the ERS-2 tape recorder problem in mid 2003. DLR receives and process in near-real-time GOME data from Matera, Miami, Beijing, Hobart, Miami, and on campaign basis from DLR station at O'Higgings. Fig. 2 shows the station coverage for ERS-2.

Fig. 2. GOME/ERS-2 station coverage (courtesy W. Lengert, ESRIN).

2. THE GDP 4.0 ALGORITHM

2.1 DOAS algorithm in GDP 4.0

In DOAS fitting, the basic model is the Beer-Lambert extinction law for trace gas absorbers [2]. An external polynomial closure term accounts for broadband effects: molecular scattering, aerosol scattering and absorption and reflection from the Earth's surface. We also include additive spectra for Ring effect interference and for undersampling. The fitting model is then:

$$Y(\lambda) \equiv \ln\left[\frac{I_\lambda(\Theta)}{I_\lambda^0(\Theta)}\right] = -\sum_g E_g(\Theta)\sigma_g(\lambda) - \sum_{j=0}^{3} \alpha_j \left(\lambda - \lambda^*\right)^j - \alpha_R R(\lambda) - \alpha_U U(\lambda) \quad (1)$$

Here, I_λ is the earthshine spectrum at wavelength λ, I_λ^0 the solar spectrum, $E_g(\Theta)$ the effective slant column density of gas g along geometrical path Θ, $\sigma_g(\lambda)$ is the associated trace gas absorption cross section. The second term in Eq.1 is the closure polynomial (a cubic filter has been assumed), with λ^* a reference wavelength for this polynomial. The last two terms on the right hand side of Eq.1 are the additive terms for the Ring reference spectrum $R(\lambda)$ and the undersampling spectrum $U(\lambda)$. The fitting minimizes the weighted least squares difference between measured and simulated optical densities $Y_{meas}(\lambda)$ and $Y_{sim}(\lambda)$ respectively.

GDP 4.0 uses the latest released version of the GOME Flight Model cross-sections (O_3 and NO_2), the so-called GOME FM98 data [3,4]. Shift and squeeze parameters may be applied to cross-section wavelength grids to improve wavelength registration against Level 1 spectra. Experience with DOAS in the operational GDP processor has shown that fitting of such non-linear parameters on a pixel-by-pixel basis can sometimes leads to numerical instability. In GDP 4.0, trace gas cross-sections are corrected for the solar I_0 effect, and have been re-sampled based on a shift of +0.016 nm (towards longer wavelengths) before use in the operational processing (no squeeze has been applied). This optimized pre-shift value has removed a systematic positive bias of 1.5 % in GDP 3.0 total ozone. Before GDP 3.0, temperature dependence in the ozone Huggins bands was specified through a single effective temperature T_{eff} chosen externally from climatology. It was found that DOAS fitting for GOME total ozone achieves greater accuracy when two ozone cross-sections at different temperatures are used as reference spectra [5]. The effective temperature T_{eff} is then retrieved in addition to the slant column. In GDP 3.0, a positive bias of 10-20 K (depending on orbit) was observed in T_{eff} when compared with values derived from temperature profiles extracted from meteorological data. GDP 4.0 has largely removed this bias (Fig.3).

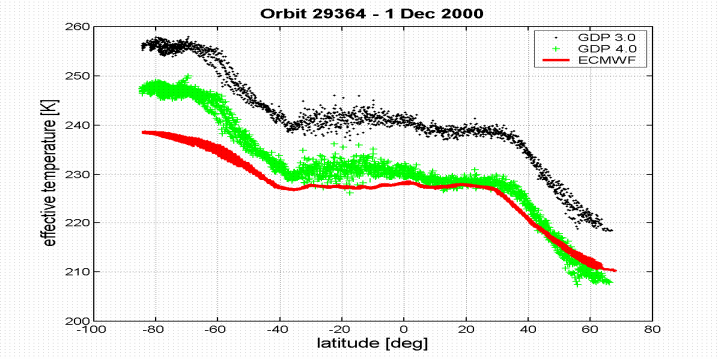

Fig. 3. DOAS-retrieved effective temperature for O_3 cross-sections from GDP V3.0 (dots) and GDP V4.0 (green), and compared with a value derived from ECMWF analysis data (solid red lines) for one GOME orbit from 1st Dec. 2000.

In GDP 4.0, the solar spectrum is used as the wavelength reference. Shift and squeeze parameters are applied to each Earthshine wavelength grid in order to re-sample the Earthshine spectrum. The GOME earthshine and solar spectra are produced by the GDP level 0-to-1 algorithm by means of the Level 0-to-1b extractor [6,7]. To improve the wavelength calibration of the level-1 spectra, we apply window-dependent pre-shifts to parts of the solar spectrum before each orbit of data is processed. These pre-shifts are established by cross-correlation with a high-resolution solar spectrum [8] over limited wavelength ranges covering the fitting window (325-335 nm for O_3 and 425-450 for NO_2 in the visible).

2.2 Air Mass Factor and vertical column computations in GDP 4.0

The ozone AMF definition that has been used in all GDP versions is the traditional one:

$$A = \frac{\log\left(I_{nog} / I_g\right)}{\tau_{vert}}, \quad (2)$$

where I_g is the radiance for an atmosphere including ozone as an absorber, I_{nog} is the radiance for an ozone-free atmosphere and τ_{vert} is the vertical optical thickness of ozone. For GOME scenarios, computation of the vertical column density (VCD) has always proceeded via the relation:

$$V = \frac{E + \Phi G A_{cloud}}{(1-\Phi)A_{clear} + \Phi A_{cloud}}, \tag{3}$$

where E is the DOAS-retrieved slant column, A_{clear} the clear sky AMF, A_{cloud} the AMF for the atmosphere down to the cloud-top level, and the "ghost column" G is the quantity of ozone below the cloud-top height. This formula assumes the independent pixel approximation for cloud treatment. In GDP 3.0, Φ is the fractional cloud cover c_f. In GDP 4.0, we use the "intensity-weighted cloud fraction" [9].

AMFs depend on ozone profiles through the radiative transfer model. In traditional DOAS retrievals, the ozone AMF depends on a fixed ozone profile taken from climatology; one application of Eq.3 yields the VCD. In the iterative approach to AMF calculation, we use a *column-classified ozone profile climatology* to establish a unique relationship between the ozone profile and its corresponding total column amount. The AMF values are now considered to be functions of the VCD through this profile-column relation, and the above formula in Eq.3 is used to update the VCD value according to:

$$V^{(n+1)} = \frac{E + \Phi G^{(n)} A^{(n)}_{cloud}}{(1-\Phi)A^{(n)}_{clear} + \Phi A^{(n)}_{cloud}} \tag{4}$$

Here, the (n) superscript indicates the iteration number. The AMFs $A^{(n)}_{clear}$ and $A^{(n)}_{cloud}$, and the ghost column $G^{(n)}$, depend on the value of VCD $V^{(n)}$ at the n^{th} iteration step. In this iteration, the slant column E reflects the true state of the atmosphere and acts as a constraint on the iteration. Eq.4 is applied repeatedly until the relative change in $V^{(n)}$ is less than a prescribed small number ε (3-5 iterations are usually sufficient). The first guess choice V_0 comes from a zonally-averaged total column climatology derived from many years of TOMS data.

For NO_2, the algorithm is simpler; there is no AMF/VCD iteration, and no molecular Ring correction: the DOAS slant column fitting result is used directly in the AMF conversion to the vertical column.

The ozone profile-column map

GDP 4.0 uses the column-classified ozone profile data set that was developed for TOMS Version 8 [10]. This climatology has a more sophisticated classification scheme than its predecessor, with 12 monthly profiles in 18 latitude zones at 10º intervals. The TV8 data has a variable column classification, from 3-5 columns at tropical latitudes and as much as 11 columns for polar regions. Column amounts vary from 125 DU to 575 DU and are separated at 50 DU intervals. For each GOME pixel, it is necessary to adjust the lowest-layer partial column to account for the actual surface pressure. For the computation of AMFs to cloud-top, the lowest layer is bounded by the cloud-top pressure, and the corresponding partial column will also scale with the logarithmic pressure drop. The ghost column is the difference between clear and cloudy sky total columns, and it emerges directly from the profile-column mapping.

Radiative Transfer calculation

In GDP 4.0 we use the LIDORT radiative transfer model [11] to simulate backscatter radiances I_g and I_{nog} in the AMF definition in Eq.2. LIDORT is a multiple scatter multi-layer discrete ordinate radiative transfer code. The atmosphere is assumed stratified into a number of optically uniform layers. The LIDORT code used here neglects light polarization. Although polarization in RT simulations is an important consideration for ozone profile algorithms, in DOAS retrievals with narrow fitting windows in the UV, the polarization signature is subsumed in the closure polynomial. A pseudo-spherical (P-S) approximation is sufficiently accurate for AMF computations with solar zenith angle (SZA) up to 90° and for line-of-sight viewing angles up to 30-35° from the nadir. However, the P-S implementation is not accurate enough for the polar-view mode of GOME (scan angles in the range 40-50°). This requires additional corrections for beam attenuation along curved line-of-sight paths, and for this we use the LIDORT Version 2.2+ [12] which possesses this line-of-sight correction.

For DOAS applications with optically thin absorbers, the trace gas AMF wavelength dependence is weak and it is customary to choose the mid-point wavelength of the fitting window. This does not apply to ozone in the 325-335 nm DOAS fitting window, and for GDP versions up to and including 3.0, the O_3 AMF was always calculated at 325.0 nm [13]. Further testing of the AMF wavelength choice was done using simulated Level 1 GOME radiances in [14], and it was shown that with this choice of 325.0 nm, total ozone errors of up to 5% are possible for solar zenith angles in excess of 80°, and generally, errors at the 0.5-1% level are found for sun angles < 80°. In the same study, it was shown that these errors are reduced (to the 1-2% level for SZA> 80°) when 325.5 nm is used as the representative AMF wavelength (Fig.4). The ozone vertical column error displayed in Fig.4 (lower panel) includes all basic aspects of the DOAS retrieval approach adopted for GDP 4.0 (except for cloud effects), and can be regarded as the "best-case "accuracy that can be expected from actual GOME retrievals. Errors below 1% are obtained in all typical GOME observation conditions, which is compliant with requirements on GOME total ozone accuracy, given the size of error sources in actual measuring conditions.

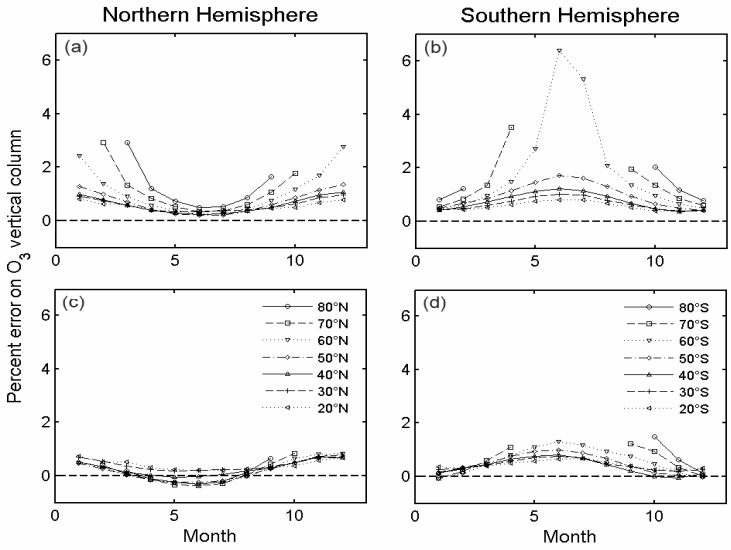

Fig 4. Impact on the total ozone accuracy of the choice of single wavelength for ozone AMF computations. Retrievals were made using synthetic radiance data based on the ozone profile climatology of *Fortuin and Kelder* [19]. Panels (a) and (b): percentage error on total ozone columns for AMFs calculated at 325.0 nm. Panels (c) and (d): percentage error on total ozone with AMFs at 325.5 nm.

The surface albedo has a large effect on the AMF. The static surface albedo climatology used in GDP 3.0 has been replaced in GDP 4.0 with a dynamic albedo data set derived from accumulated satellite reflectance data [9]. We use a combination of the GOME Lambertian equivalent reflectivity (LER) data set of albedos prepared from 5.5 years of reflectivity data [15], and the Nimbus-7 TOMS LER data set prepared from 14.5 years of data from 1978 [16], and valid for 340 and 380 nm. In GDP 4.0 total ozone retrievals, aerosols are neglected in the AMF computations, since AMF and VCD values are insensitive to aerosols to first order. The aerosol sensitivity issue is described in more detail in [9].

In the independent pixel approximation, cloud information is reduced to the specification of 3 parameters (cloud fraction, cloud-top albedo and cloud-top pressure). Clouds are regarded as highly reflecting Lambertian surfaces. GDP 4.0 employs the OCRA and ROCINN cloud pre-processing steps before the total column retrieval. OCRA uses the GOME sub-pixel PMD output and it delivers the geometric cloud fraction [17]. ROCINN [18] is a new fitting algorithm using O_2 *A* band reflectivities from GOME, and it retrieves cloud-top pressure and cloud-top albedo. Cloud fraction in the ROCINN algorithm is constrained to take the OCRA value when the algorithms are used in tandem.

2.3 Molecular Ring correction

The smoothing ("filling-in") of Fraunhofer features in zenith sky spectra has become known as the Ring effect. It is now known to be caused in large part by inelastic rotational Raman scattering (RRS) from air molecules. The Ring reference spectrum is defined as the change in optical depth between intensities calculated with and without RRS. The Ring effect is generally small, as RRS contributes only 4% of all scattering by air molecules. However, modulations of

backscattered light in the ozone Huggins bands are also large enough for inelastic RRS effects to appear as the filling-in of ozone absorption features (the molecular or telluric Ring effect). Spectral dependence in this molecular Ring effect correlates quite strongly with the behaviour of the ozone absorption.

The Ring effect is treated as "pseudo-absorber" interference in the DOAS algorithm using a Ring reference spectrum as additive fitting parameter in Eq.1. It was found that neglect of the telluric Ring effect in GDP 3.0 leads to systematic underestimation of ozone total columns (up to 10%) [14]. From this study, a correction for the molecular Ring effect in ozone retrieval was developed. Considering only O_3 absorption, the correction is based on a simplified forward model of the intensity at satellite *I(λ)* which includes an explicit contribution due to inelastic RRS:

$$I(\lambda) = I^0(\lambda) \cdot \exp\left[-\sigma_{O3}(\lambda) \cdot E_{O3} - P_1^\lambda\right] + E_{Ring} \cdot I_0^{RRS}(\lambda) \cdot \exp\left[-\sigma_{O3}(\lambda) \cdot E_{O3}^{RRS} - P_2^\lambda\right]. \quad (5)$$

The first term on the right-hand follows the Lambert-Beer law for ozone absorption, with $I^0(\lambda)$ the solar intensity, and σ_{O3} and E_{O3} the ozone absorption cross-section and effective slant column respectively. Elastic scattering effects are subsumed by means of the low band pass polynomial P_1^λ. The Ring effect is modeled by the second term in Eq.5, in which there are several approximations. First, it is assumed that Raman-scattered light is generated close to the surface of the atmosphere, with the spectral shape given by a source spectrum for Raman scattering $I_0^{RRS}(\lambda)$. This source spectrum only treats the spectral smoothing effect of RRS on the solar intensity. In practice it is calculated by the convolution of a GOME irradiance spectrum using Raman cross sections appropriate to inelastic scattering into the wavelength of interest. The fractional intensity of Raman light (the E_{Ring} parameter) is freely adjustable. This may vary considerably and will depend on parameters such as cloud coverage, cloud altitude and surface albedo. Ozone absorption (the term $\sigma_{O3}(\lambda).E_{O3}^{RRS}$) is then treated consistently, assuming that Raman photons produced at the surface and/or above clouds travel upward to the satellite. Ozone absorption taking place in the incoming light is assumed to be fully smeared out in the inelastic process, so that it can be neglected in the first approximation.

Eq.5 can be rewritten (after a Taylor expansion, discarding higher-order terms) in the following way:

$$\ln\left[\frac{I(\lambda)}{I^0(\lambda)}\right] = -\sigma_{O3}(\lambda).E_{O3}^{'} - \sigma_{Ring}(\lambda).E_{Ring} - P(\lambda), \quad (6)$$

with the Ring cross-section $\sigma_{Ring}(\lambda)$ defined as:

$$\sigma_{Ring}(\lambda) = -\frac{I_0^{RRS}(\lambda)}{I^0(\lambda)}. \quad (7)$$

Eq.6 is the familiar DOAS fitting model, from which E'_{O3}, E_{Ring} and the $P(\lambda)$ polynomial coefficients can be derived in the usual manner. The major difference with Ring correction methods used in previous studies comes in the definition of the modified O_3 effective slant column E'_{O3}, which is related to the effective slant column for *elastic* scattering (E_{O3}) by the following formula:

$$E_{O3}^{'} \cong E_{O3} \cdot \left\{1 + E_{Ring} \cdot \overline{\sigma}_{Ring} \cdot \left(1 - \frac{\sec(\theta_0)}{A_{total}}\right)\right\} = E_{O3}.M_{Ring}, \quad (8)$$

where A_{total} is the ozone AMF, θ_0 the solar zenith angle, and $\overline{\sigma}_{Ring}$ an average Ring cross-section calculated over the spectral fitting interval. In this formulation, the DOAS fitting is essentially unchanged, and it gives fitted parameters E'_{O3} and E_{Ring}. The effective slant column for ozone is then adjusted *after* the fit through the relation $E_{O3} = M_{Ring}\, E'_{O3}$. We use the LIDORT-calculated total AMF already computed at each AMF/VCD iteration step to obtain M_{Ring} and the corrected slant column $E'_{O3} = E_{O3} / M_{Ring}$ as required for the VCD update (Eq.4). The accuracy of our simplified approach has been tested under various conditions using the same SCIATRAN model as a reference. In Fig.5, errors on the retrieved ozone slant columns are compared for retrievals performed with a basic "Fraunhofer-only" Ring correction (as in GDP 3.0), and retrievals using the new correction method developed for GDP 4.0. The underestimation in the absence of molecular Ring correction lies in the range 5-10% and shows clear solar zenith angle dependence. This systematic underestimation is largely compensated by the new correction, for all conditions applied in the tests.

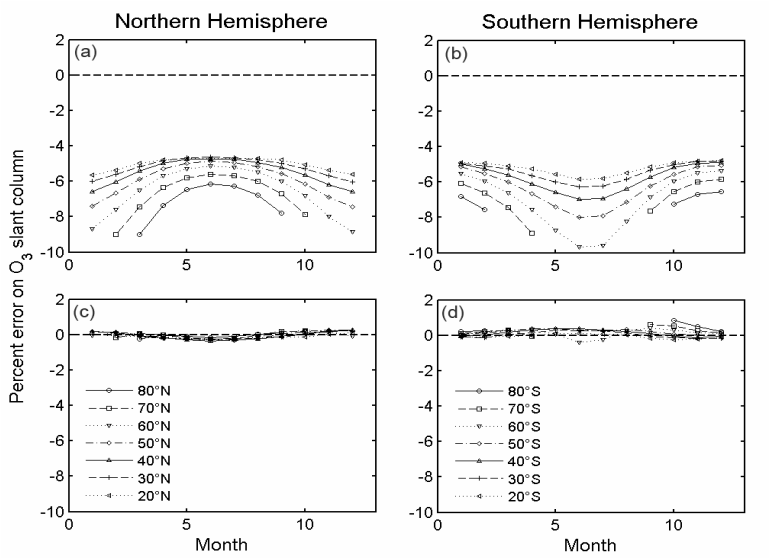

Fig. 5 Ring effect tests using synthetic data calculated with the SCIATRAN model, based on the ozone profile climatology of *Fortuin and Kelder* [19]. Top panels: percentage error on retrieved ozone slant column when not accounting for molecular filling-in (GDP 3.0 baseline). Bottom panels: percentage error on retrieved slant columns after application of the new Ring effect treatment (GDP 4.0 baseline).

2.4 Accuracy and stability issues for GDP 4.0 algorithm

An external geophysical validation of total ozone product showed that the total ozone accuracy reached by GDP 4.0 is at the *percentage level*, i.e. it is comparable to the accuracy of the ground-based instruments [20]. An estimation of the error budget of the GDP 4.0 algorithm is provided in [9].

The long-term stability of the GOME total ozone record is a key consideration for trend analysis. In Fig.6, monthly mean ozone differences between GDP 4.0 and Brewer measurements at Hohenpeissenberg are shown for a 10-year period from July 1995 through April 2005. A sine function has been fitted to the time series in order to highlight seasonal variations in the differences. The amplitude of these variations is about 0.5% and the mean bias is 0.3%. The long-term stability of GOME and the absence of any significant time-dependent bias are clear. It is worth noting that the stability is still evident after more than 8 years, despite some loss of ozone accuracy from June 2003 to December 2004 caused by the absence of daily solar calibration measurements in the GOME Level 1 product during that period (this problem has been solved in the updated GOME Level 1 processor).

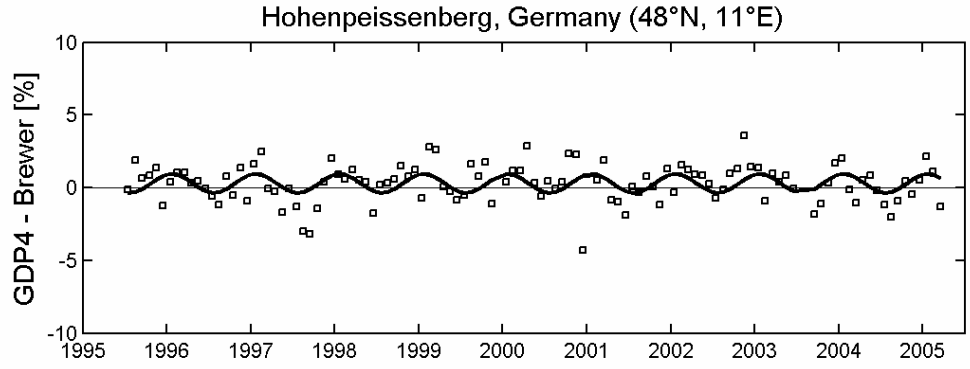

Fig 6. GDP 4 – Hohenpeissenberg Brewer monthly mean ozone differences from July 1995 until April 2005. A sinusoidal fit to the time series (thick black line) highlights the size of seasonal variations in the differences (amplitude: 0.5%). The mean bias over the 10-year time period is 0.3%.

3. OPERATIONAL PRODUCTS

The GDP 4.0 level 2 operational products of GOME comprise total columns of ozone and NO_2, as well as cloud products: cloud fraction, cloud-top height, cloud-top albedo. The following images show some examples of the GOME products, including the development of the ozone hole and cloud time series.

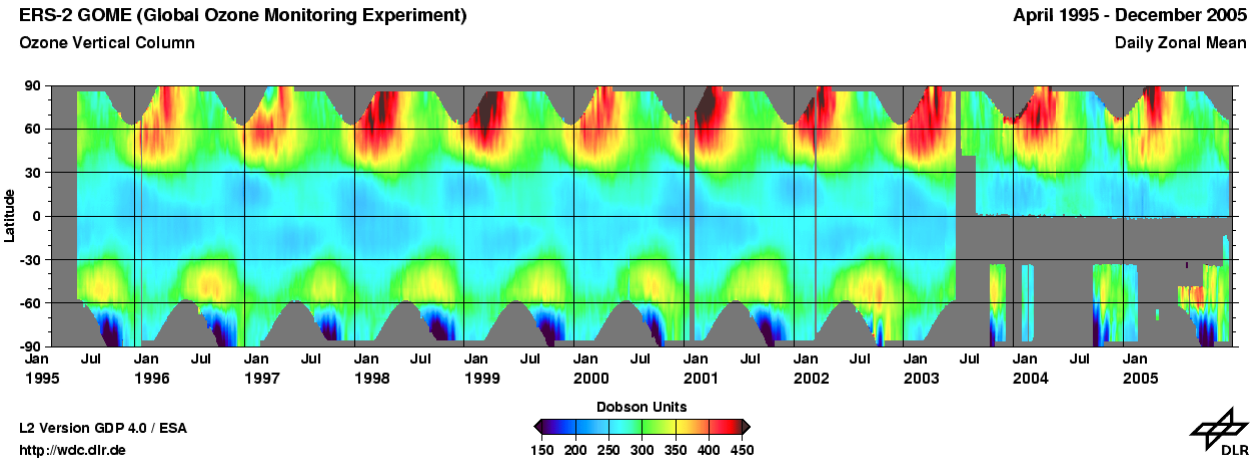

Fig.7. Time series of ozone daily latitudinal averages computed with the GOME data from June 1995 to December 2005. Note the data discontinuity since June 2003 due to the ERS-2 tape recorder failure.

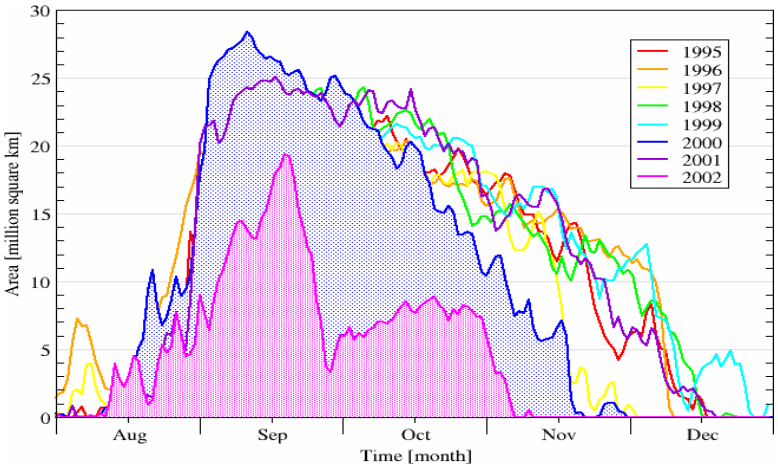

Fig. 8. Development of the Antarctic ozone hole area from 1995 to 2002 (courtesy T. Erberseder, DLR-DFD).

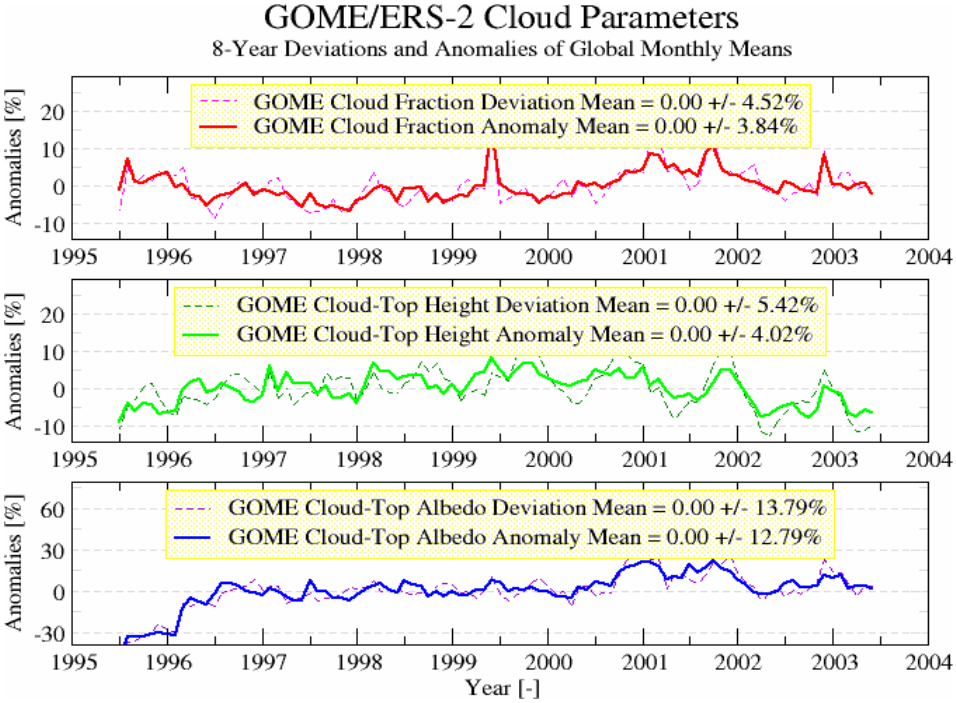

Fig. 9. Global monthly mean deviations and anomalies of GOME derived cloud parameters.

Acknowledgements
The authors would like to thank to all DFD and IMF colleagues that make possible the success of the GDP project, as well as the partners from BIRA, RT Solutions, AUTH, Universities of Bremen and Heidelberg, KNMI, RAL, SAO, SRON, and NASA.

REFERENCES

1. Loyola D., Balzer W., Aberle B., Bittner M., Kretschel K., Mikusch E., Muehle H., Ruppert T., Schmid C., Slijkhuis S., Spurr R., Thomas W., Wieland T., Wolfmueller M., "Ground Segment for ERS-2/GOME Sensor at the German D-PAF", 3rd ERS Scientific Symposium, Florence, Italy, pp. 591-596, March 1997.
2. Spurr, R., D. Loyola, W. Thomas, W. Balzer, E. Mikusch, B. Aberle, S. Slijkhuis, T. Ruppert, M. Van Roozendael, J.-C. Lambert, and T. V. Soebijanta (2005), GOME Level 1-to-2 Data Processor Version 3.0: A Major Upgrade of the GOME/ERS-2 Total Ozone Retrieval Algorithm, *Applied Optics*, 44, 7196-7209, 2005.
3. Burrows, J., A. Dehn, B. Deters, S. Himmelmann, A. Richter, S. Voigt, and J. Orphal, Atmospheric Remote-Sensing Reference Data from GOME: Part 1. Temperature-dependent absorption cross-sections of NO_2 in the 231-794 nm range, *J. Quant. Spectrosc. Radiat. Trans.*, *60*, 1025-1031, 1998.
4. Burrows, J., A. Richter, A. Dehn. B. Deters, S. Himmelmann, S. Voigt, and J. Orphal, Atmospheric remote sensing reference data from GOME: Part 2. Temperature-dependent absorption cross-sections of O_3 in the 231-794 nm range, *J. Quant. Spectrosc. Radiat. Transfer*, *61*, 509-517, 1999.
5. Richter, A., and J. Burrows, Tropospheric NO_2 from GOME measurements, *Adv. Space Res.*, *29*, 1673-1683, 2002.
6. Aberle, B., W. Balzer, A. von Bargen, E. Hegels, D. Loyola and R. Spurr, GOME Level 0 to 1 Algorithms Description, Tech. Note ER-TN-DLR-GO-0022 (Issue 5/B), Deutsches Zentrum für Luft und Raumfahrt, Oberpfaffenhofen, Germany, 2002.
7. Slijkhuis, S., B. Aberle, and D. Loyola, GOME Data Processor Extraction Software User's Manual, ER-SUM-DLR-GO-0045, 2004.
8. Chance, K., and R. Spurr, Ring effect studies: Rayleigh scattering including molecular parameters for rotational Raman scattering, and the Fraunhofer spectrum, *Applied Optics*, *36*, 5224-5230, 1997.
9. Van Roozedael, M., et al., Ten years of GOME/ERS-2 total ozone data: the new GOME Data Processor (GDP) Version 4.0: I. Algorithm Description, *J. Geophys. Res.*, in press, 2006.
10. Bhartia, P. K., Algorithm Theoretical Baseline Document, TOMS v8 Total ozone algorithm, 2003.

11. Spurr, R. J. D., T. P. Kurosu, and K. V. Chance, A Linearized discrete Ordinate Radiative Transfer Model for Atmospheric Remote Sensing Retrieval, *J. Quant. Spectrosc. Radiat. Transfer*, *68*, 689-735, 2001.
12. Spurr, R., LIDORT V2PLUS: a comprehensive radiative transfer package for nadir viewing spectrometers, remote Sensing of clouds and atmosphere, Proceedings SPIE conference 5235, Barcelona, Spain., 2003.
13. Burrows, J., M. Weber, M. Buchwitz, V. Rozanov, A. Ladstätter-Weißenmayer, A. Richter, R. de Beek, R. Hoogen, K. Bramstadt, K.-U. Eichmann, M. Eisinger, and D. Perner, The Global Ozone Monitoring Experiment (GOME): mission concept and first scientific results, *J. Atmos. Sci*, *56*, 151-175, 1999.
14. Van Roozendael, M., V. Soebijanta, C. Fayt, and J.-C. Lambert, Investigation of DOAS Issues Affecting the Accuracy of the GDP Version 3.0 Total Ozone Product, in ERS-2 GOME GDP 3.0 Implementation and Delta Validation, Ed. J.-C. Lambert, ERSE-DTEX-EOAD-TN-02-0006, ESA/ESRIN, Frascati, Italy, Chap.6, pp.97-129, 2002.
15. Koelemeijer, R. B. A., J. F. de Haan, J. W. Hovenier, and P. Stammes, A database of spectral surface reflectivity in the range 335-772 nm derived from 5.5 years of GOME observations, *J. Geophys. Res.*, *108*, 2003.
16. Herman, J. R, and E. A. Celarier, Earth surface reflectivity climatology at 340 nm to 380 nm from TOMS data, *J. Geophys. Res*., *102*, 28003-28011, 1997.
17. Loyola, D., and T. Ruppert, A new PMD cloud-recognition algorithm for GOME, *ESA Earth Observation Quarterly*, *58*, 45-47, 1998.
18. Loyola, D., Automatic Cloud Analysis from Polar-Orbiting Satellites using Neural Network and Data Fusion Techniques, *IEEE International Geoscience and Remote Sensing Symposium*, 4, 2530-2534, Alaska., 2004.
19. Fortuin, J. P. F., and H. Kelder, An ozone climatology based on ozonesonde and satellite measurements, *J. Geophys. Res.*, *103*, 31709-31734., 1998.
20. Balis et al., Ten years of GOME/ERS-2 total ozone data: the new GOME Data Processor (GDP) Version 4.0: II. Ground-based validation and comparison with TOMS V7/V8, *J. Geophys. Res.*, in press 2006